

Exploring complex normal faulting systems through physics-based dynamic rupture modeling

Cycle Team Meeting

Hugo S.

Institut de Recherche pour le Développement IRD - ISTerre

O., Scotti, S., Hok, A.-A. Gabriel and T. Taufiqurrahman

ANR EQTIME Project

May 12, 2022

Motivation

Preliminary exploration

Preliminary conclusions & discussion

On going work and to dos!

My skills

- Static & Kinematic coseismic modeling/inversion

My skills

- Static & Kinematic coseismic modeling/inversion
- Monitoring seismic activity

My skills

- Static & Kinematic coseismic modeling/inversion
- Monitoring seismic activity
- Dynamic seismic source modeling

My skills

- Static & Kinematic coseismic modeling/inversion
- Monitoring seismic activity
- **Dynamic seismic source modeling**

Motivation

Seismic Hazard in Central Italy

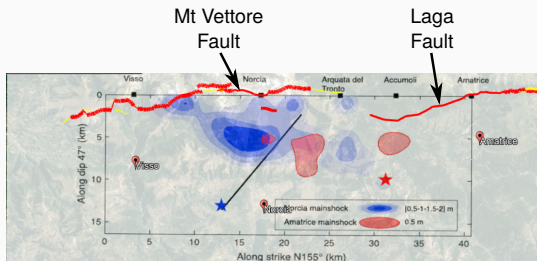
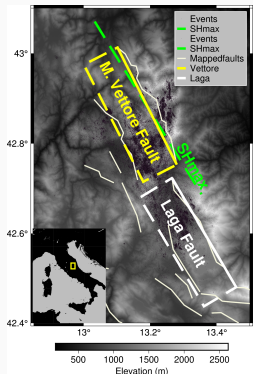


Figure 11. Comparison between the slip distributions imaged on the VBFS fault during the 24 August (red contours; Tinti et al., 2016) and the 30 October 2016 main shocks (blue contours; this study) projected on the same fault striking 155° and dipping 47°. The red and blue stars are the two main shocks hypocentral locations. The black line is the intersection of the N210° segment and the N155° fault.



Modified by O. Scotti from Scognamiglio et al. (2018)

Seismic Hazard in Central Italy

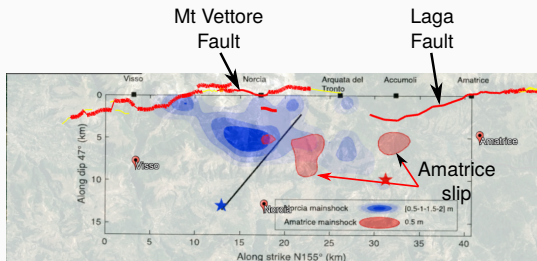
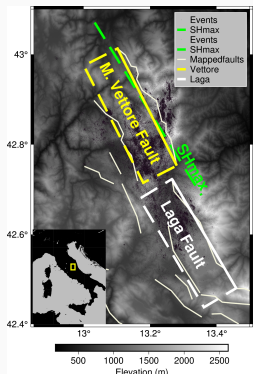


Figure 11. Comparison between the slip distributions imaged on the VBFS fault during the 24 August (red contours; Tinti et al., 2016) and the 30 October 2016 main shocks (blue contours; this study) projected on the same fault striking 155° and dipping 47°. The red and blue stars are the two main shocks hypocentral locations. The black line is the intersection of the N210° segment and the N155° fault.



Modified by O. Scotti from Scognamiglio et al. (2018)

Seismic Hazard in Central Italy

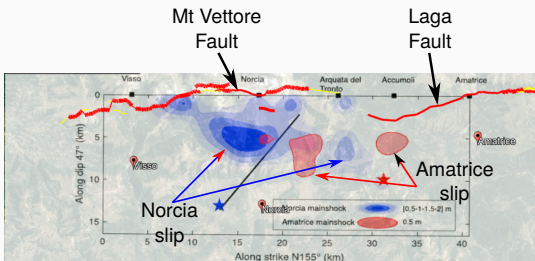
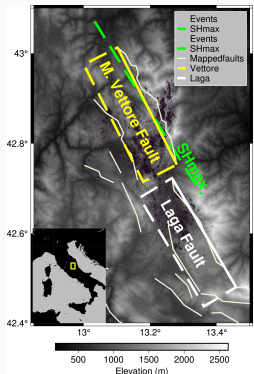


Figure 11. Comparison between the slip distributions imaged on the VBFS fault during the 24 August (red contours; Tinti et al., 2016) and the 30 October 2016 main shocks (blue contours; this study) projected on the same fault striking 155° and dipping 47°. The red and blue stars are the two main shocks hypocentral locations. The black line is the intersection of the N210° segment and the N155° fault.



Modified by O. Scotti from Scognamiglio et al. (2018)

Seismic Hazard in Central Italy

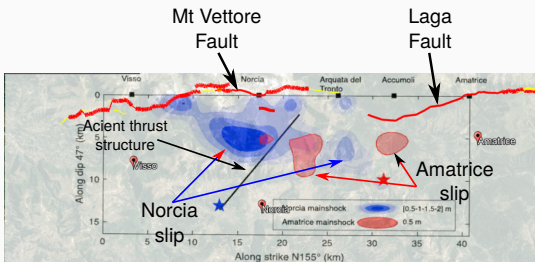
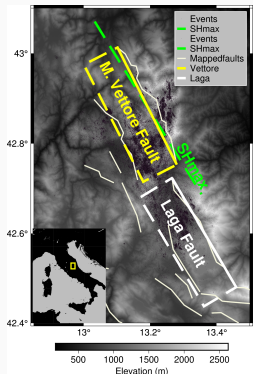


Figure 11. Comparison between the slip distributions imaged on the VBFS fault during the 24 August (red contours; Tinti et al., 2016) and the 30 October 2016 main shocks (blue contours; this study) projected on the same fault striking 155° and dipping 47°. The red and blue stars are the two main shocks hypocentral locations. The black line is the intersection of the N210° segment and the N155° fault.



Modified by O. Scotti from Scognamiglio et al. (2018)

Seismic Hazard in Central Italy

Rupture jump across step-overs

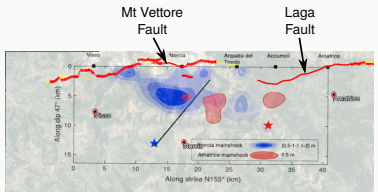


Figure 11. Comparison between the slip distributions imaged on the VBFS fault during the 24 August (red contours; Tinti et al., 2016) and the 30 October 2016 main shocks (blue contours; this study) projected on the same fault striking 155° and dipping 47°. The red and blue stars are the two main shocks hypocentral locations. The black line is the intersection of the N21°W segment of the VBFS and the N155° fault.

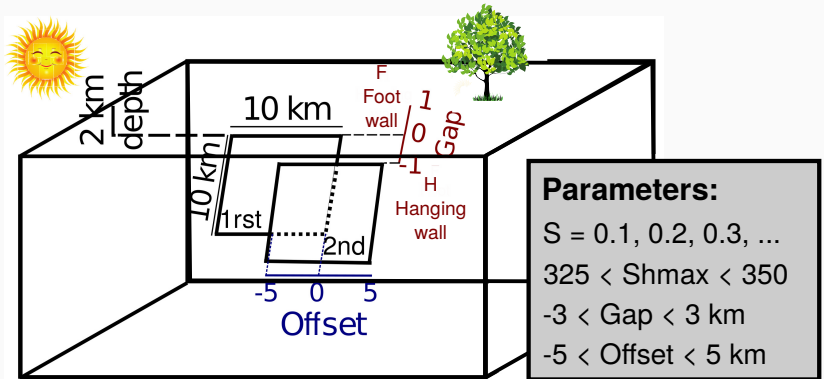
- Potential larger magnitudes?
- Conditions promoting this?
 - Geometry
 - Stress conditions
- To enhance SHA!

Investigate the physical conditons
promoting rupture jumps across step overs
regarding normal fault systems

Previous studies focused on strike-slip fault systems: Galis et al. (2015); Hu et al. (2016); Bai and Ampuero (2017); Li and Liu (2020); Oglesby (2008), and more ...

Preliminary exploration

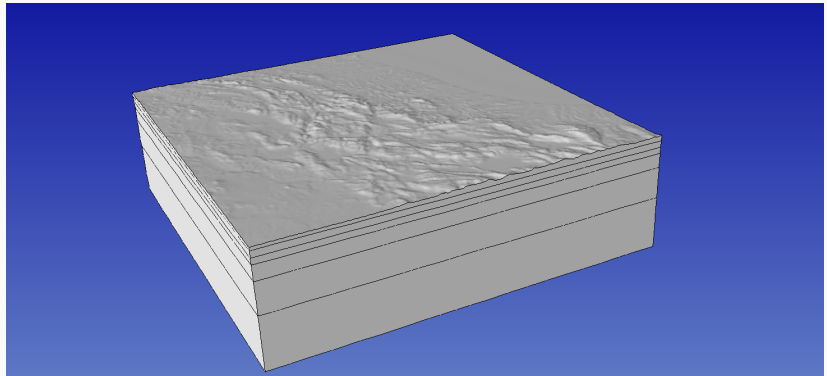
Preliminary exploration: Geometry and settings

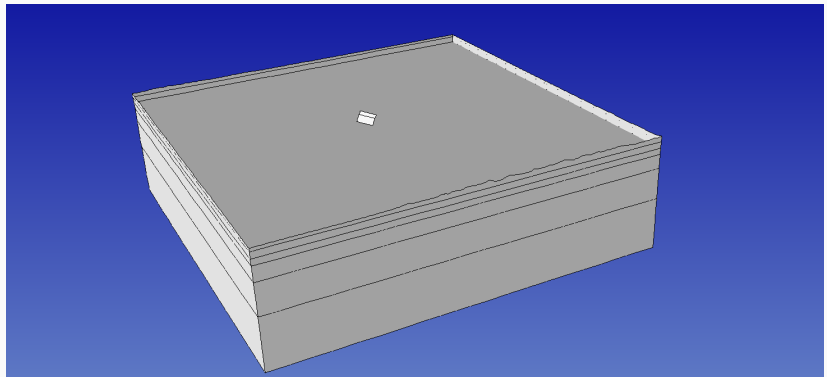


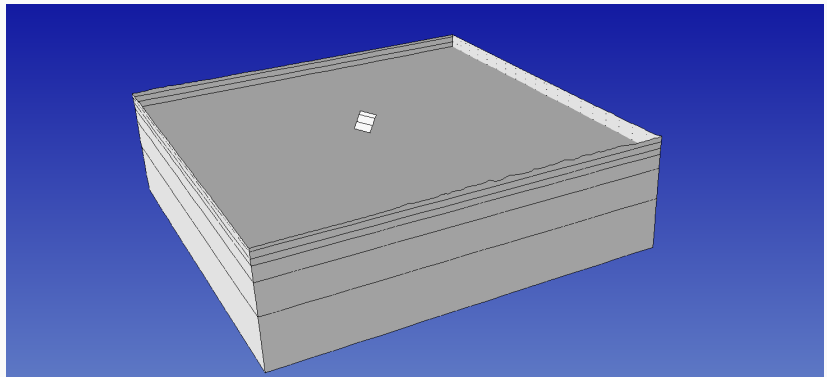
(www.seissol.org; e.g., Wollherr et al., 2018; Ulrich et al., 2019)

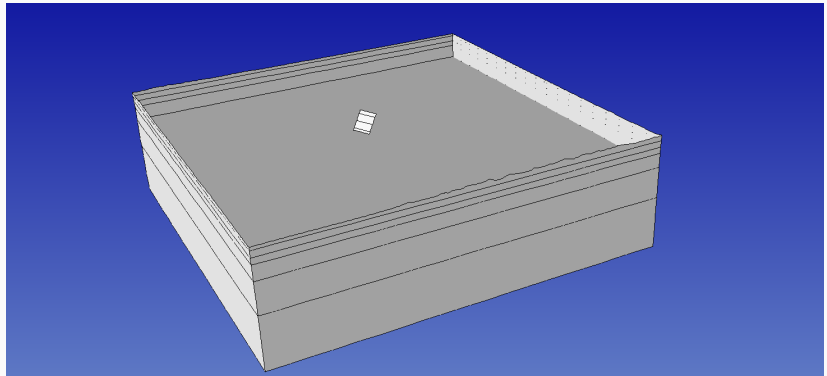
SMALL PUBLICITÉ !!

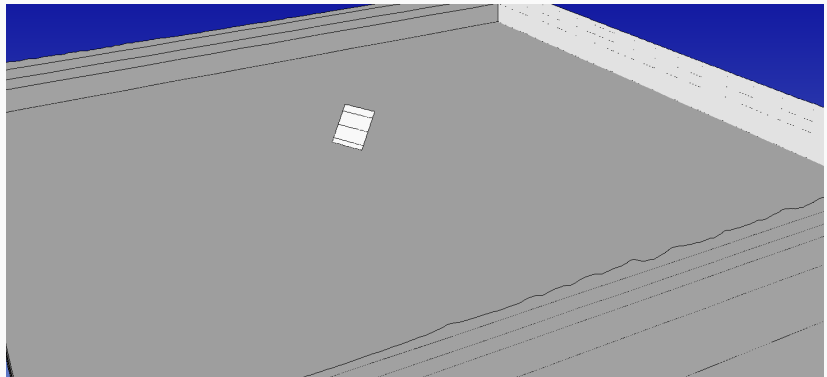
SimModeler: meshing engine
&
SeisSol: dynamic rupture modeling

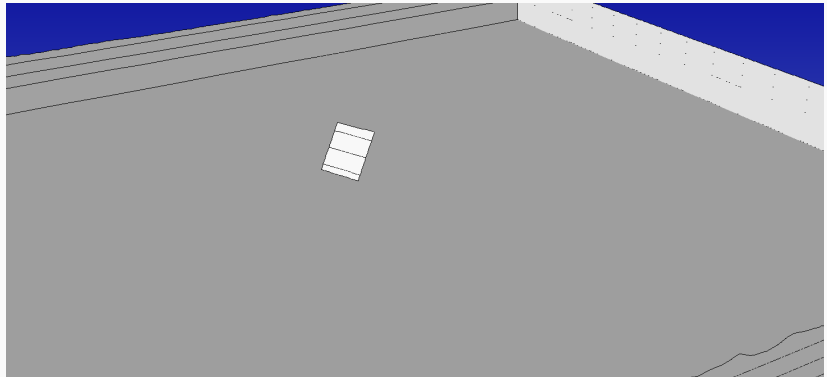


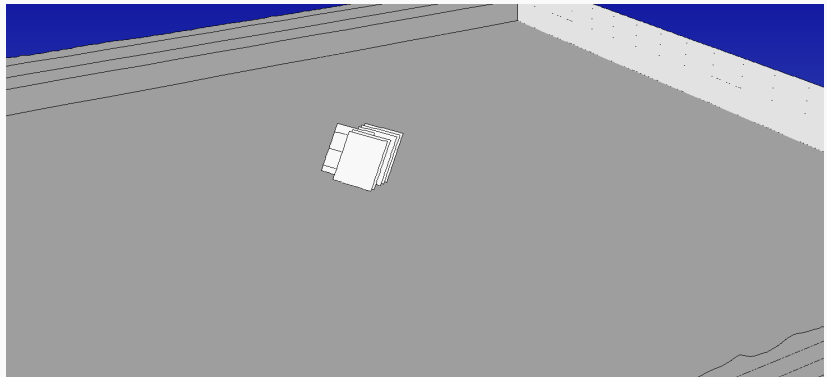


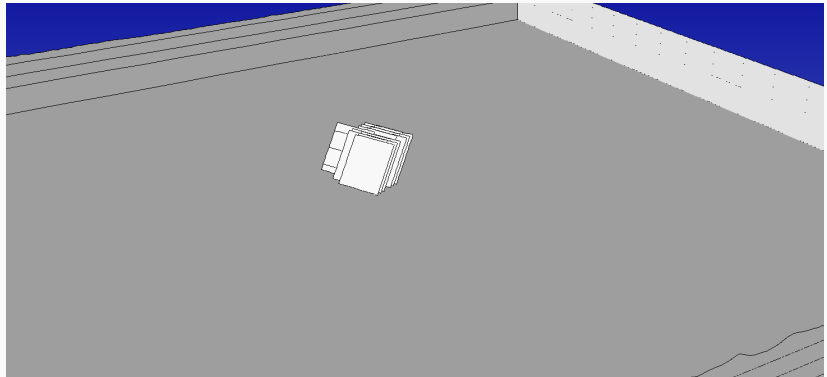


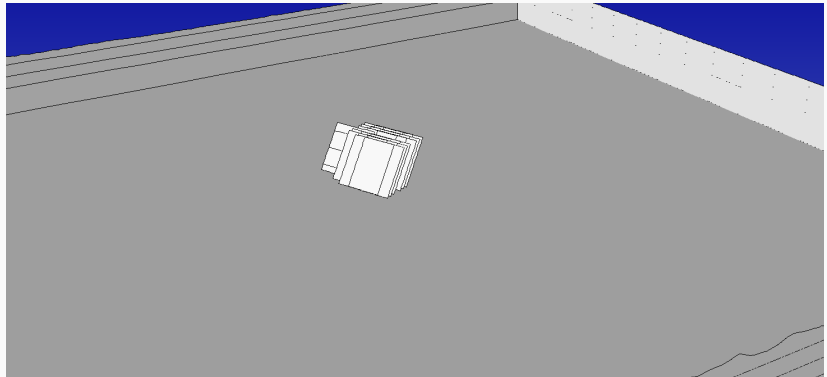


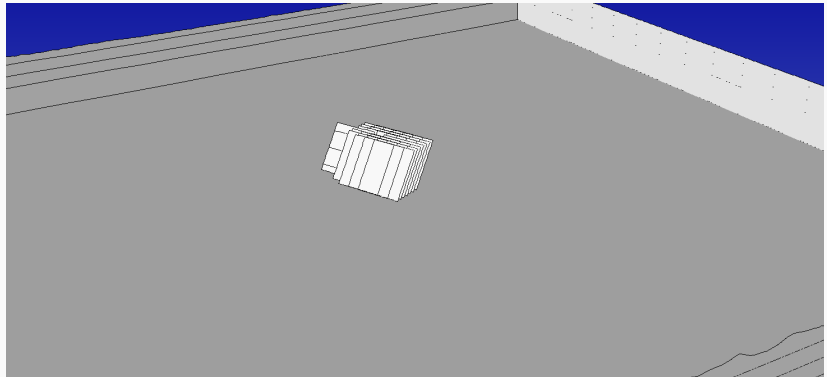


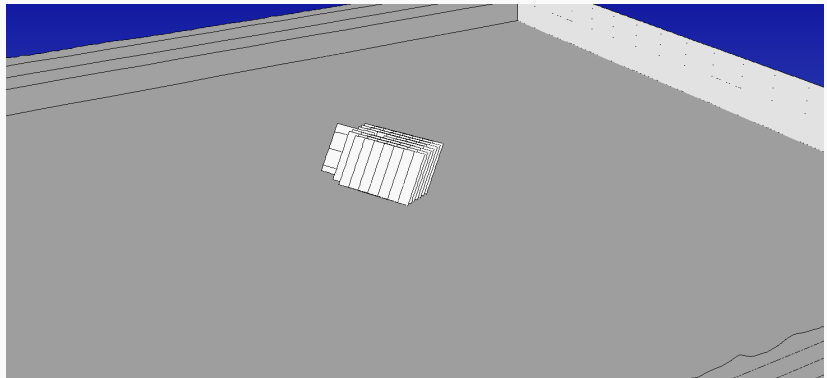


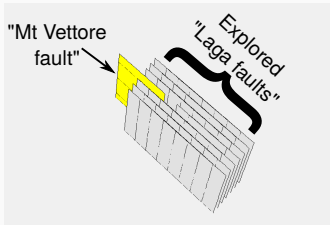






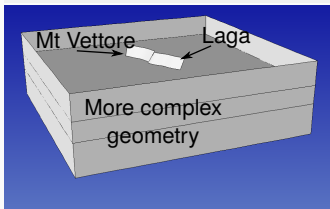


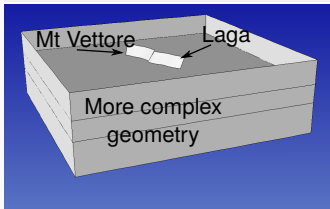
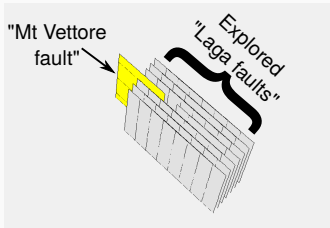




SimModeler & SimModSuite

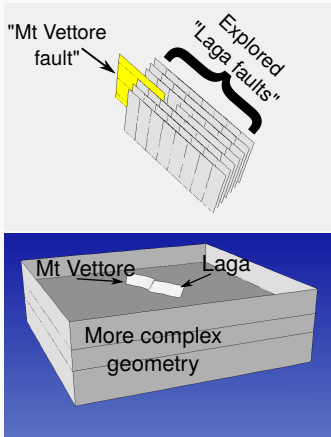
- Complex mesh & fault geometries





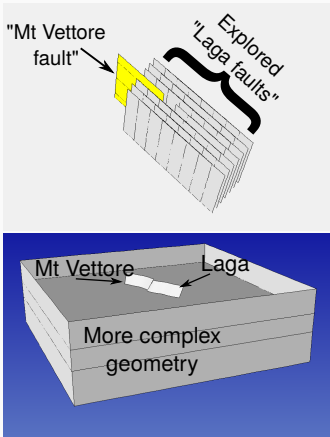
SimModeler & SimModSuite

- Complex mesh & fault geometries
- Mesh adaptivity



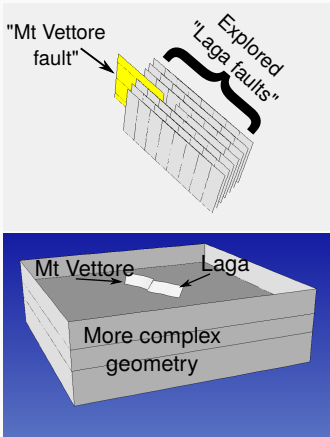
SimModeler & SimModSuite

- Complex mesh & fault geometries
- Mesh adaptivity
- Simple user-friendly interface



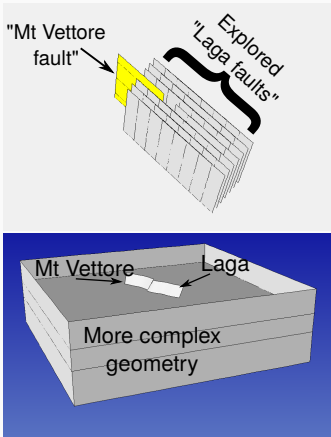
SimModeler & SimModSuite

- Complex mesh & fault geometries
- Mesh adaptivity
- Simple user-friendly interface
- Academic **Free** License



SimModeler & SimModSuite

- Complex mesh & fault geometries
- Mesh adaptivity
- Simple user-friendly interface
- Academic **Free** License
- Available documentation

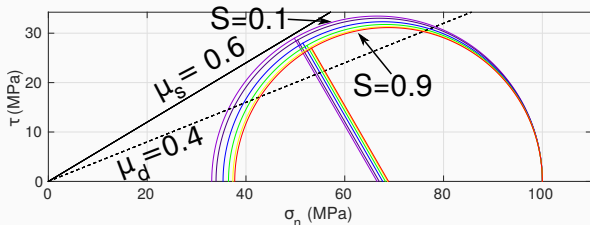


SimModeler & SimModSuite

- Complex mesh & fault geometries
- Mesh adaptivity
- Simple user-friendly interface
- Academic **Free** License
- Available documentation
- Currently being installed on
IST-OAR ... Thanks Jean-Noel!

SeisSol dynamic rupture engine:

Preliminary exploration: Stress conditions



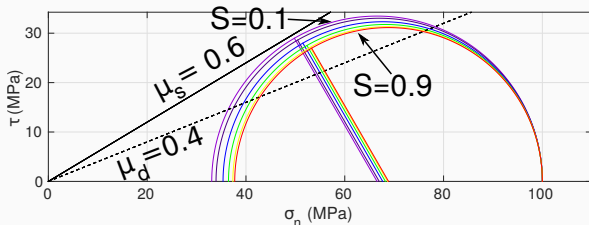
Stress-Strength dimensionless ratio

$$S = \frac{\tau_p - \tau_o}{\tau_o - \tau_r}$$

Stress & medium conditions

- Stress levels explored
- $S = 0.1, 0.2, 0.4, 0.6, 0.8, 0.9$

Preliminary exploration: Stress conditions



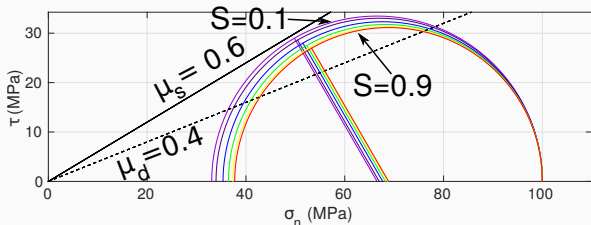
Stress-Strength dimensionless ratio

$$S = \frac{\tau_p - \tau_o}{\tau_o - \tau_r}$$

Stress & medium conditions

- Stress levels explored
 $S = 0.1, 0.2, 0.4, 0.6, 0.8, 0.9$
- Linear Slip Weakening:
 $\mu_s = 0.6, \mu_d = 0.4, d_c = 0.15 \text{ m}$

Preliminary exploration: Stress conditions



Stress-Strength dimensionless ratio

$$S = \frac{\tau_p - \tau_0}{\tau_0 - \tau_r}$$

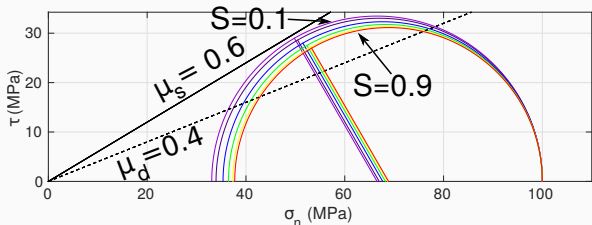
Stress & medium conditions

- Stress levels explored
 $S = 0.1, 0.2, 0.4, 0.6, 0.8, 0.9$
- Linear Slip Weakening:
 $\mu_s=0.6, \mu_d=0.4, d_c=0.15$ m
- Slow rupture initiation

$$\mu_s \xrightarrow{t \rightarrow 1} \mu_d$$

at a 4×4 km² patch

Preliminary exploration: Stress conditions



Stress-Strength
dimensionless
ratio

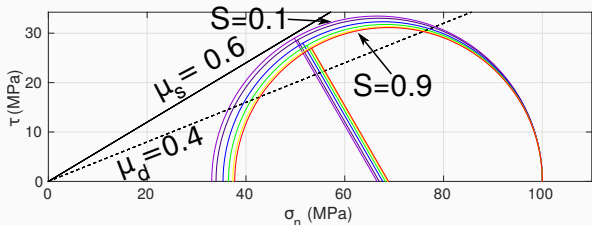
$$S = \frac{\tau_p - \tau_0}{\tau_0 - \tau_r}$$

Stress & medium conditions

- Stress levels explored
 $S = 0.1, 0.2, 0.4, 0.6, 0.8, 0.9$
- Linear Slip Weakening:
 $\mu_s = 0.6, \mu_d = 0.4, d_c = 0.15 \text{ m}$
- Slow rupture initiation
$$\mu_s \xrightarrow{t \rightarrow 1} \mu_d$$

at a $4 \times 4 \text{ km}^2$ patch
- σ_{zz} depth-dependent
$$\sigma_{zz} = (\rho - 1 \times 10^3) * g * \min(-1.5 \times 10^3, z)$$

Preliminary exploration: Stress conditions



Stress-Strength
dimensionless
ratio

$$S = \frac{\tau_p - \tau_o}{\tau_o - \tau_r}$$

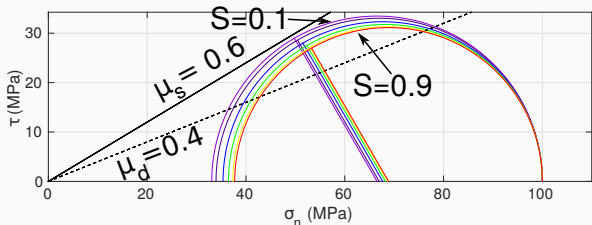
Stress & medium conditions

- Stress levels explored
 $S = 0.1, 0.2, 0.4, 0.6, 0.8, 0.9$
- Linear Slip Weakening:
 $\mu_s=0.6, \mu_d=0.4, d_c=0.15$ m
- Slow rupture initiation
- σ_{zz} depth-dependent
$$\sigma_{zz} = (\rho - 1 \times 10^3) * g * \min(-1.5 \times 10^3, z)$$
- Layered medium from Tinti et al. (2021)

$$\mu_s \xrightarrow{t \rightarrow 1} \mu_d$$

at a 4×4 km² patch

Preliminary exploration: Stress conditions



Stress-Strength
dimensionless
ratio

$$S = \frac{\tau_p - \tau_o}{\tau_o - \tau_r}$$

Stress & medium conditions

- Stress levels explored
 $S = 0.1, 0.2, 0.4, 0.6, 0.8, 0.9$
- Linear Slip Weakening:
 $\mu_s=0.6, \mu_d=0.4, d_c=0.15$ m
- Slow rupture initiation
 $\mu_s \xrightarrow{t \rightarrow 1} \mu_d$
at a 4×4 km² patch
- σ_{zz} depth-dependent
$$\sigma_{zz} = (\rho - 1 \times 10^3) * g * \min(-1.5 \times 10^3, z)$$
- Layered medium from Tinti et al. (2021)
- Faults share same stress level

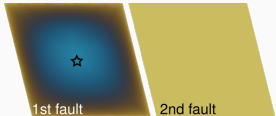
Preliminary exploration: 3 different cases

For these cases: Gap = 1 km, Offset = 1 km

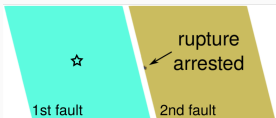
Only 1 fault segment breaks

S : 0.6

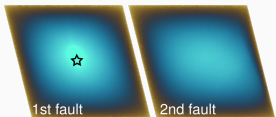
Preliminary exploration: 3 different cases



- Only 1st fault breaks



- Rupture arrested on the 2nd fault

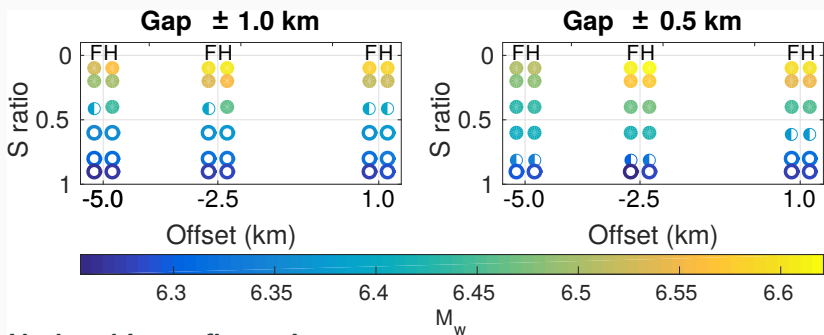


- Both faults break

3 Different cases

Preliminary exploration: Results from simulations

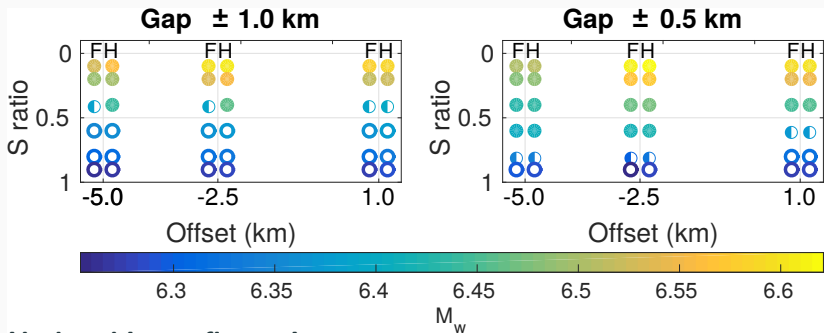
72 simulations: [4] Gap values \times [3] Offset values \times [6] Stress levels



Under this configuration:

Preliminary exploration: Results from simulations

72 simulations: [4] Gap values \times [3] Offset values \times [6] Stress levels

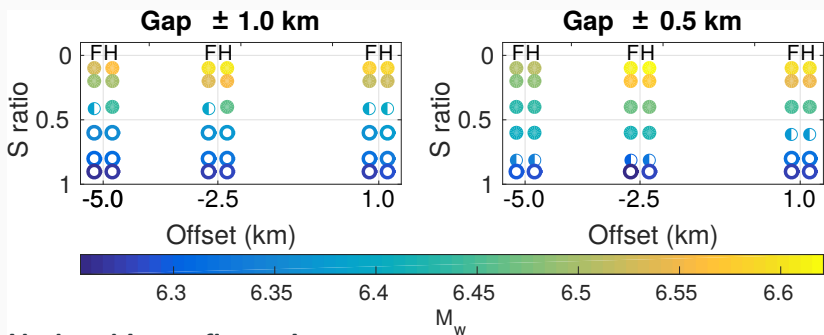


Under this configuration:

S depends only on the stress level and not on μ_s or μ_d .

Preliminary exploration: Results from simulations

72 simulations: [4] Gap values \times [3] Offset values \times [6] Stress levels



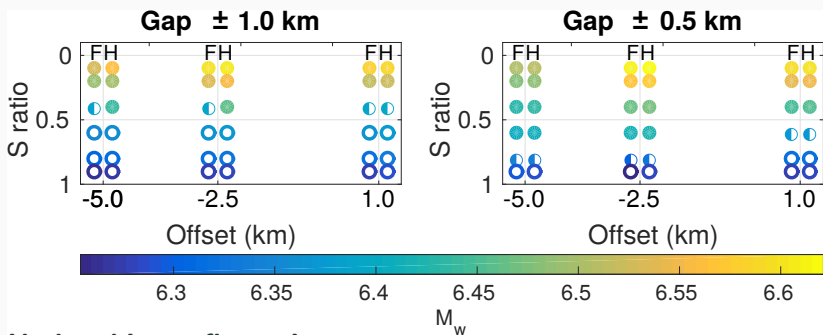
Under this configuration:

S depends only on the stress level and not on μ_s or μ_d .

Rupture is arrested mainly due to the pre-stress level of faults.

Preliminary exploration: Results from simulations

72 simulations: [4] Gap values \times [3] Offset values \times [6] Stress levels



Under this configuration:

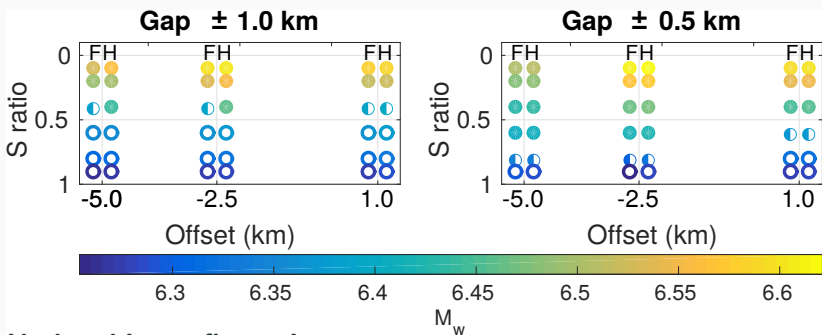
S depends only on the stress level and not on μ_s or μ_d .

Rupture is arrested mainly due to the pre-stress level of faults.

Beyond > 1 km offset jumps might be expected only at low S -ratio levels.

Preliminary exploration: Results from simulations

72 simulations: [4] Gap values \times [3] Offset values \times [6] Stress levels



Under this configuration:

S depends only on the stress level and not on μ_s or μ_d .

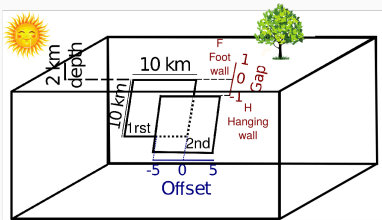
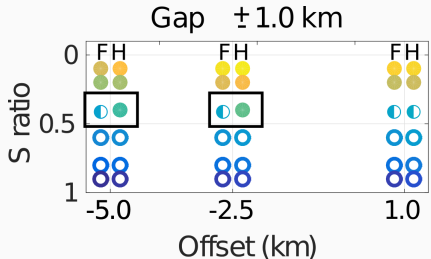
Rupture is arrested mainly due to the pre-stress level of faults.

Beyond > 1 km offset jumps might be expected only at low S -ratio levels.

Stress shadow and hanging/foot wall asymmetry are observed.

Preliminary conclusions & discussion

Hanging/foot wall behavioral asymmetry

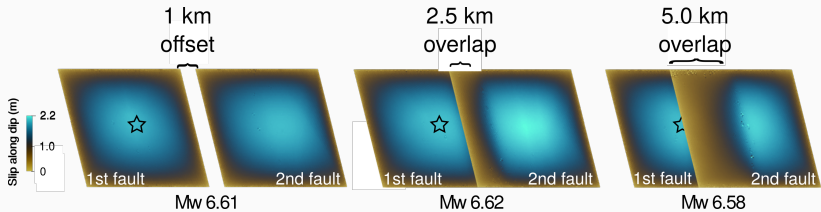


Triggering potential:

When the 2nd fault is located on the hanging wall (with respect to the 1st fault) the dynamically triggered rupture is more likely to be self-sustainable (break away).

Stress shadow: Slip VS Fault Proximity

For these cases: Gap = 0.5 km, $S = 0.1$

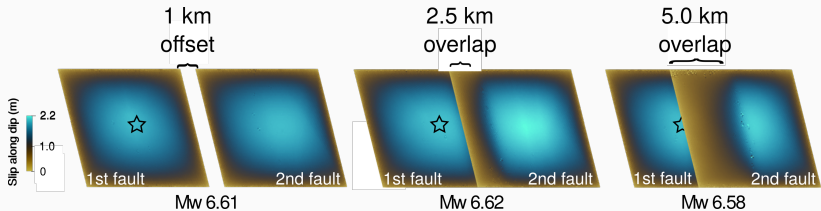


Slip VS Fault Proximity:

The final slip distribution (estimated energy) increases/decreases according to the distance between faults.

Stress shadow: Slip VS Fault Proximity

For these cases: Gap = 0.5 km, $S = 0.1$



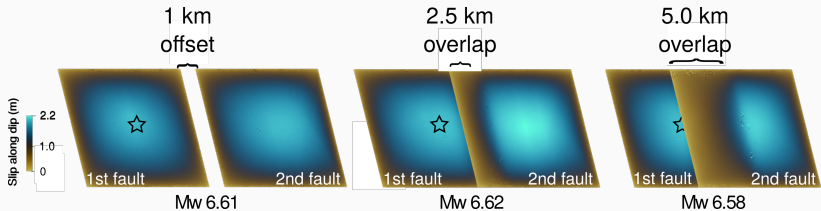
Slip VS Fault Proximity:

The final slip distribution (estimated energy) increases/decreases according to the distance between faults.

Large overlap → Fault proximity → high triggering effect
but,

Stress shadow: Slip VS Fault Proximity

For these cases: Gap = 0.5 km, $S = 0.1$



Slip VS Fault Proximity:

The final slip distribution (estimated energy) increases/decreases according to the distance between faults.

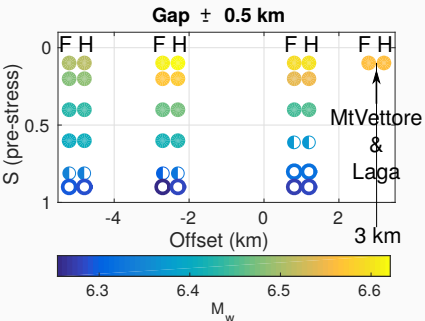
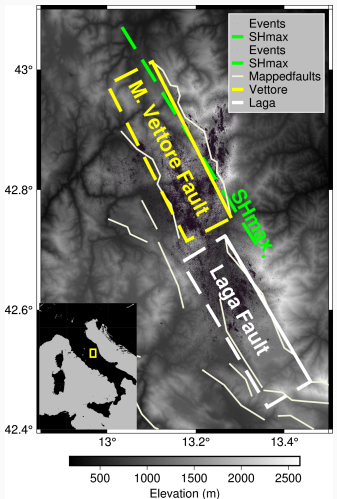
Large overlap → Fault proximity → high triggering effect but,

Stress shadow → decreases slip distribution on 2nd fault

On going work and to dos!

Central Italy complex normal faulting system

Mapped fault traces



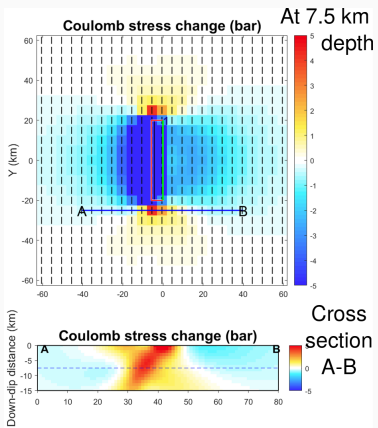
Central Italy:

- ☞ Extensional regime
- ☞ Multi-segment normal faulting system
- ☞ Complex fault geometry
- ☞ Seismicity along one or several segments
 - 1980 Ms6.9 Irpinia
 - 2016 Amatrice-Visso-Norcia

Static or Dynamic triggered?

Static Coulomb Stress Change (1 fault only!)

On going:



- More simulations covering larger distances (>5 km)
- Estimation of dynamic stress changes
- Linking simulations with real case
- Writing results!

References

References

- Aochi, H. (2018). Dynamic asymmetry of normal and reverse faults due to constrained depth-dependent stress accumulation. *Geophysical Journal International*, 215(3):2134–2143.
- Bai, K. and Ampuero, J.-P. (2017). Effect of seismogenic depth and background stress on physical limits of earthquake rupture across fault step overs. *Journal of Geophysical Research: Solid Earth*, 122(12):10–280.
- Faure Walker, J., Boncio, P., Pace, B., Roberts, G., Benedetti, L., Scotti, O., Visini, F., and Peruzza, L. (2021). Fault2sha central apennines database and structuring active fault data for seismic hazard assessment. *Scientific data*, 8(1):1–20.
- Galis, M., Pelties, C., Kristek, J., Moczo, P., Ampuero, J.-P., and Mai, P. M. (2015). On the initiation of sustained slip-weakening ruptures by localized stresses. *Geophysical Journal International*, 200(2):890–909.
- Hu, F., Zhang, Z., and Chen, X. (2016). Investigation of earthquake jump distance for strike-slip step overs based on 3-d dynamic rupture simulations in an elastic half-space. *Journal of Geophysical Research: Solid Earth*, 121(2):994–1006.
- Li, G. and Liu, Y. (2020). Earthquake rupture through a step-over fault system: An exploratory numerical study of the leech river fault, southern vancouver island. *Journal of Geophysical Research: Solid Earth*, 125(11):e2020JB020059.
- Oglesby, D. (2008). Rupture termination and jump on parallel offset faults. *Bulletin of the Seismological Society of America*, 98(1):440–447.
- Scognamiglio, L., Tinti, E., Casarotti, E., Pucci, S., Villani, F., Cocco, M., Magnoni, F., Michelini, A., and Dreger, D. (2018). Complex fault geometry and rupture dynamics of the mw 6.5, 30 october 2016, central italy earthquake. *Journal of Geophysical Research: Solid Earth*, 123(4):2943–2964.
- Ulrich, T., Vater, S., Madden, E. H., Behrens, J., van Dinther, Y., Van Zelst, I., Fielding, E. J., Liang, C., and Gabriel, A.-A. (2019). Coupled, physics-based modeling reveals earthquake displacements are critical to the 2018 palu, sulawesi tsunami. *Pure and Applied Geophysics*, 176(10):4069–4109.
- Wollherr, S., Gabriel, A.-A., and Uphoff, C. (2018). Off-fault plasticity in three-dimensional dynamic rupture simulations using a modal discontinuous galerkin method on unstructured meshes: implementation, verification and application. *Geophysical Journal International*, 214(3):1556–1584.